Optimum electrostatic force control for fabricating a hybrid UV-curable aspheric lens

2010 J. Micromech. Microeng. 20 075001

(http://iopscience.iop.org/0960-1317/20/7/075001)

J. Micromech. Microeng. **20** (2010) 075001 (7pp) doi:10.1088/0960-1317/20/7/075001

Optimum electrostatic force control for fabricating a hybrid UV-curable aspheric lens*

Kuo-Yung Hung[1,6,7], Liang-Wei Chang[2], Fan-Gang Tseng[3,4,7,8], Jin-Chern Chiou[5] and Yi Chiu[5]

[1] Institute of Mechanical and Electrical Engineering, Ming-Chi University of Technology, Taiwan, Republic of China
[2] Department of Engineering and System Science, National Tsing Hua University, Taiwan, Republic of China
[3] Engineering and System Science Department/NanoEngineering and MicroSystems Institute, National Tsing Hua University, Taiwan, Republic of China
[4] Division of Mechanics, Research Center for Applied Sciences, Academia Sinica, Taiwan, Republic of China
[5] Department of Electrical Engineering, National Chiao Tung University, Taiwan, Republic of China

E-mail: kuoyung@mail.mcut.edu.tw and fangang@ess.nthu.edu.tw

Received 12 March 2010, in final form 15 April 2010
Published 21 May 2010
Online at stacks.iop.org/JMM/20/075001

Abstract

The purpose of this paper is to use a hybrid structure and the electrostatic force to fabricate aspheric lenses with high optical transmittance (95% at 405 nm). The hybrid structure is composed of Norland Optical Adhesive 63 (NOA63) (refractive index: 1.5802 at 405 nm) and BK-7 glass (refractive index: 1.5302). OSLO (Optics Software for Layout and Optimization) and CFD (Computational Fluid Dynamics) software packages were used to simulate the electric field gradient between the top and bottom electrodes and to produce the optimum bottom electrode design. Different electrode designs were also tested in order to optimize the morphology of the lens profile. The resulting lens profiles have clear apertures of approximately 0.92 mm with maximum shape errors of less than 0.18% and the spot size of the fabricated aspheric lenses can be controlled to approximately 0.504 μm. This technology can be used as a generic approach to fabricate lenses for applications in various micro-optical systems.

(Some figures in this article are in colour only in the electronic version)

Introduction

A single aspheric lens has been considered in the application of inexpensive consumer cameras, laser diode collimation and for coupling light into and out of optical fibers due to their low cost and good performance. In addition, a single aspheric lens has also been considered in the application of optical data storage systems, because of its low aberration, small size, high numerical aperture and short focal length. Small glass or plastic aspheric lenses can be made by molding technologies [1–3], which allow low-cost mass production. Larger aspheric lenses are fabricated by grinding and polishing. They can be prepared by point-contact contouring to roughly the right profiles which are then polished to their final shape. Aspheric surfaces can also be made by polishing with a small tool with a compliant surface that conforms to the optic, although precise control of the surface profile and quality is difficult and the

* Partially based on the following paper, orally presented at IEEE NEMS 2010 conference: Hung K-Y, Chang L-W, Tseng F-G and Hang N T M 2010 Optimum electrostatic-force control for fabricating a hybrid UV-curable aspheric lens *5th IEEE Int. Conf. on Nano/Micro Engineered and Molecular Systems (Xiamen, China, 20–23 January 2010)*.
[6] Member, IEEE 41513443.
[7] Author to whom any correspondence should be addressed.
[8] Member, IEEE.

results may change as the tool wears. Single-point diamond turning is an alternate process, in which a computer-controlled lathe uses a diamond tip to directly cut the desired profile into a piece of glass or another optical material. Diamond turning is slow and has limitations in the materials on which it can be used and on the surface accuracy and smoothness that can be achieved.

Recently, Hung *et al* [4] have proposed to use gradient electrostatic force attraction to produce micro-aspheric lenses, followed by UV cure forming. However, the use of SU-8 (MicroChem Corp., USA) in such applications is limited because the polymer has poor transmittance over a 405 nm light wavelength. Ordinary plastic materials such as polymethylmethacrylate (PMMA), polycarbonate (PC) and polybutadiene-styrene (PBS) are not suitable to be employed in the aforementioned method since they are solid at room temperature and cannot be shaped by electrostatic force and UV curing.

An electrostatic modulation is usually used in liquid zoom lens fabrication. For example, Philips Inc. [5] proposed the use of electrowetting of oil and water and applied the electric field while changing the contact angle of the oil and water. This shapes the curvature of the lens to achieve the lens profile modulation, or, to refer the dielectric electrophoresis methodology [6] on two different dielectric materials, in order to achieve micro-lens zoom effects. In a dielectric lens, under a gradient electric field, the generated dielectric force causes the dielectric liquid to be shaped toward the region with the lowest electric field strength. One distinct advantage is that electrolysis, joule heating and micro-bubble formation often occur in electro-wetting lenses due to the transportation of the free electric charges and the alternating electric fields [7] but dielectric lenses do not introduce these problems; they require only a patterned electrode to generate a gradient electric field [7–10]. A non-mechanical method to form uniform liquid droplet arrays was demonstrated, but the droplets could drift in the lens cell, which degrades the lens' stability [9]. Since the drive voltage and the zoom range of a static liquid zoom lens are the main specifications, Xu *et al* [11] used parallel-plate capacitor theory with a special electrode design to reduce the voltage required for a zoom lens, and the electrostatic force was based on the mechanism of non-contact modulation to fabricate an aspheric lens. If a polymer is used as the material for a 405 nm DVD lens, it might hold great promise to overcome the major bottlenecks in the production of large curvature lenses.

To overcome these limitations, this paper presents an electric-field-controlled methodology for shaping the profile of a polymer aspheric lens. By using a hybrid structure, we hope to meet the design specifications of an optical pickup head. The specifications of the designed polymer lens are listed as follows: a clear aperture of 0.92 mm, a Strehl ratio of 0.9972 and a spot size near the diffraction limit of 0.3923 μm (table 1). This paper first describes the use of OSLO (Optics Software for Layout and Optimization, Lambda Research Corporation, USA) to simulate the hybrid structure of the polymer material Norland Optical Adhesive 63, (NOA, 63, Norland Products Inc., USA) with a fixed thickness on the BK-7 glass (Schott, USA) substrate to obtain the best optical properties and aspheric parameters. Then, numerical estimation of the volume required for the lens is explained for precise volume quantification (error ~1%). During the manufacturing process, parallel-plate electrode modulation is used to facilitate the change on the curvature of the high-order aspheric lens. The calculations on various parameters of the lens morphology are presented after the use of the lens curve-fitting mechanism and the error of the lens morphology in the experiment is compared with the design value. Finally, the use of a blue laser diode (405 nm) for spot measurements of the aspheric lens to assess the optical effect and quality of the lens is described.

Table 1. The simulation parameters and optical results of the hybrid lens by OSLO.

Optical specification	NOA63 + BK7
BK7 index (405 nm)	1.530 239
NOA63 index (405 nm)	1.5802
C1	2.18
C2	0
Conic constant	−0.63
Fourth order	−0.034 02
Sixth order	0.214 99
Eighth order	−0.901 86
Optical performance	
NA	0.53
Strehl ratio	0.9972
Working distance (mm)	0.385 377
Spot size on diffraction limit (μm)	0.3923

Design principle

The hybrid structure is composed of NOA 63 (refractive index is 1.5802 at 405 nm wavelength) and BK-7 glass (refractive index is 1.5302 with a thickness of 375 μm). The concept of the hybrid aspheric lens is shown in figure 1. The lens has a clear aperture of 0.92 mm and the diameter D is 1.2 mm. The transmittance of a 1 mm thick NOA63 is about 95% for the 405 nm wavelength. The BK-7 optical parameter is based on the manufacturer's specification data for the OSLO simulation. The lens simulation is considered as a monochromatic finite-conjugate system.

The aspheric equation for C1 (surface sag) in figure 1 is

$$Z = \frac{(c = 2.18)r^2}{1 + \sqrt{1 - (c = 2.18)^2((k = -0.63) + 1)r^2}} + (c_1 = -0.034\ 02)r^4 + (c_2 = 0.214\ 99)r^6 + (c_3 = -0.901\ 86)r^8, \quad (1)$$

where Z is the sag of the aspheric surface, r is the curvature radius of the lens, c is the inverse of the radius of curvature, c_1, c_2, c_3 and c_4 are the higher order coefficients of the aspheric equation for the C1 surface (in figure 1) and k is the conic constant. This is for the single-convex lens design because the refractive index of NOA63 is 1.58 ($\lambda = 405$ nm). When the light from the optically dense medium (NOA 63) enters the optically sparse medium (BK-7), it will deviate from the normal. The deviation from the normal direction is exactly the

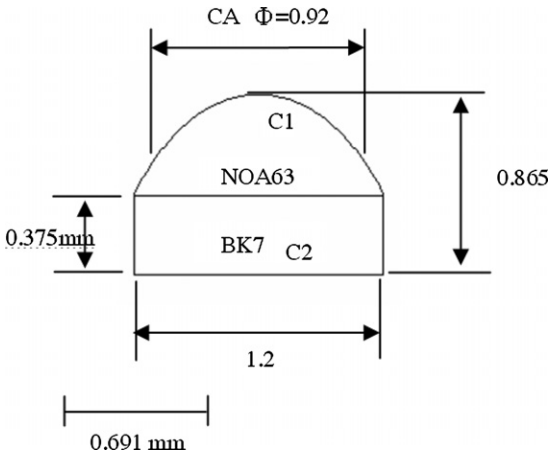

Figure 1. The specifications of the designed hybrid aspheric lens.

direction of the lens focus, therefore increasing the focusing effects of the lens and giving a shorter working distance. In addition, the spot size of the lens is mainly limited by the diffraction limit of the optics; therefore, the design presented here can fulfill the specifications of an optical DVD pickup head, and the simulated spot size (full width at half maximum, FWHM) is less than 0.4 μm. The simulation parameters and results are shown in table 1.

The system to manipulate the formation of the hybrid aspheric lens includes two electrodes in parallel: the upper electrode consists of ITO on a glass substrate while the ring-type bottom electrode (the width is $2D - d$) is patterned aluminum on the bottom glass substrate (figure 2). This means that there is no aluminum in the 'd' region in figure 2.

Here, we propose a design for the bottom electrode ($2D - d$) and use the computational fluid dynamics method to simulate the gradient electrostatic force on the lens to explore the relationship between different electrode designs ($2D - d$) and the electrostatic force distributions of the lens. The simulation parameters of NOA 63 are as follows: a density of 1200 kg m^{-3}, a resistivity of $\sim 10^{12}$ Ω cm and a dielectric coefficient ε_2 of $\sim$2.7. The air has a density of 1.1614 kg m^{-3}, a resistivity of $\sim 10^6$ Ω cm and a dielectric constant ε_1 of 1.00054. ε_0 is the permittivity of free space. F is the electrostatic force, V is the applied voltage and E is the electric field between the parallel electrodes.

From Kelvin theory (equation (2)) [12],

$$\vec{F} = \frac{\varepsilon_0}{2}(\varepsilon_1 - \varepsilon_2)\nabla(E \bullet E). \tag{2}$$

We can see that electrostatics mainly involves the difference between the medium permittivity and the distribution of the electric field gradient in the system. Based on the equation

$$E_t = \frac{\frac{V}{\varepsilon_2}}{\frac{t}{\varepsilon_2} + \frac{s-t}{\varepsilon_1}} \Rightarrow \begin{cases} (\text{edge})\, E_{t\to 0} = \frac{V\varepsilon_1}{s\varepsilon_2} \\ (\text{center})\, E_{t\to s} = \frac{\frac{V}{\varepsilon_2}}{\frac{t}{\varepsilon_2}+\frac{s-t}{\varepsilon_1}} = \frac{V}{s} \end{cases}, \tag{3}$$

the ratio of the electrostatic field E_t near the lens edge ($t \to 0$) and its central part ($t \to s$) can be found, and it is about $\varepsilon_1/\varepsilon_2$ ($\varepsilon_1 \sim 1 < \varepsilon_2 \sim 3.3$). $t(d)$ is the lens height, which is a function of d, and s is the distance between the top and bottom electrodes.

It is clear that the force at the lens center is significantly higher than that at the lens edge, and a pyramid-shaped gradient of electrostatic force is formed. Therefore, by changing the bottom electrode design, the electric field of the lens edge can be controlled. The change of the electrostatic force gradient creates different high-order aspheric lens profiles, as shown in figures 3(a)–(c). Figure 3(a) shows the system parameters used in this paper. When d is reduced, the degree of non-uniformity of the electric field at the edge of the lens is increased resulting in an increase of the electrostatic force of the lens at the edge (figure 3(b)). Normally, the degree of the non-uniformity of the electric field is determined by the distribution of the surface charge. Figure 3(c) shows the schematic diagram of the lens profile during electric field modulation when $d > D$.

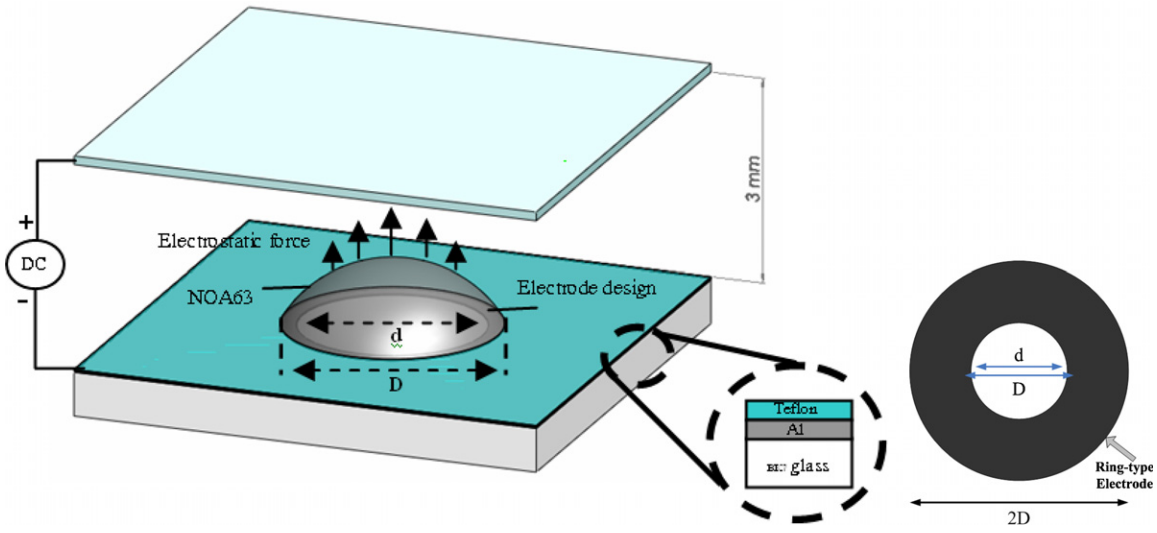

Figure 2. The concept of the hybrid aspheric lens. D is the lens diameter; ($2D - d$) is the aluminum ring width of the bottom electrode. It means that there is no aluminum in the 'd' region.

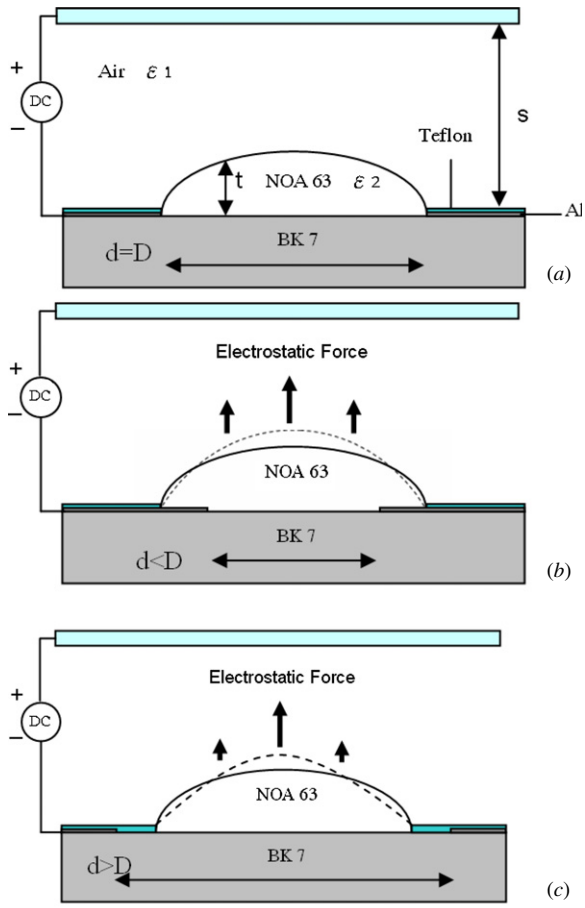

Figure 3. (*a*) The system parameters used in this paper. (*b*) The diagram of the electric field modulation lens profile when $d < D$. (*c*) A diagram of the electric field modulation lens profile when $d > D$.

Fabrication process

The principle of the optimum design is as follows. For a specific lens material with a dielectric constant ε_2, we obtain an electrostatic force F based on equation (3). Extending these equations to a lens diameter D (1.2 mm), we obtain a profile of the lens for a specific electrode design (figure 4(*a*)). The CFD method was used to discuss the relationship of the gradient electrostatic force versus the lens profile for different values of d. Figure 4(*a*) shows that the electric field at the center is stronger than that at the edge of the lens. Figure 4(*b*) shows that smaller d values (0.9 mm) correspond to stronger electrostatic forces at the edge. This makes the distribution curve of the electrostatic force smoother, i.e., if $d = 0.9$ mm $< D$, the electrostatic force distribution is similar to that shown in figure 5(*a*). Figure 5(*b*) shows the distribution for $d = 1.1$ mm $\sim D$.

The system includes two electrodes in parallel: the upper electrode is made of 1000 Å ITO on a glass substrate because the lens material NOA 63 is a photo-curable material. Based on the simulation results presented in figure 4(*b*), the fabrication process of the bottom electrode, as shown in figure 6, is presented. The detailed processing of the glass substrate begins with the patterned aluminum electrode (3000 Å) (figures 6(*a*)–(*c*)). Then, Teflon was patterned to define the lens diameter D by lift-off and for the purpose of lens self-assembly (figures 6(*d*)–(*f*)). Lens material NOA 63 was dispensed, and the volume was controlled (∼1% volume error) by a precision dispensing machine (DAJIUM Inc., 8000 series) (figure 6(*g*)). The dispensing machine was operated at 20 °C with a dispensing output gauge of 10 psi. The inner diameter of the dispensing needle is 0.11 mm, and a Teflon-coated head was used for controlling the NOA 63 volume precision. An electrostatic force was then applied for aspheric lens shaping. Finally, UV light was used to make the NOA 63 curable. Because of the low moisture content characteristics of the NOA 63, the profile changes very little during the UV exposure process. There was only about 0.05 mg weight loss during the UV exposure process. In addition, the NOA 63 volume and electrode spacing between the top and bottom were fixed. Only the applied voltage and bottom electrode diameter were varied in this paper.

Results

Figures 7(*a*)–(*c*) show the fabricated lens images obtained for d values of 0.9, 1.0 and 1.1 mm, respectively with different optimum spot sizes. For controlling the lens profile, we analyzed the shape error of the lens (in comparison with the design profile given in equation (1)) by curve fitting, and the results are shown in figure 8. The shape errors in figure 8 were calculated based on the real aspheric lens profile minus the designed profile in equation (1). It shows that the optimum parameters are $d = 1.0$ mm at 3600 V, an electrode spacer of 3 mm and a minimum shape error of 0.9 μm (0.18%). When $d = 1.1$ mm at 3600 V, a shape error of 0.588 μm was obtained. In addition, when $d = 0.9$ mm at 3600 V, a maximum shape error of 4.83 μm resulted. Normally, a larger shape error would get a more serious aberration.

Finally, the focus spot sizes of the aspherical lens illustrated in figures 7(*a*) to (*c*) are 0.84, 0.504 and 0.588 μm, respectively (analyzed by Image-Pro Plus Program). The results were compared to those of a commercial DVD double convex objective lens with a spot size of 0.42 μm (figure 7(*d*)). From figures 7 and 8, we know that the morphology of errors led to the generation of aberration and a larger spot was the result. It proves that electrode parameters could control the profile of the aspheric lens, with different numerical apertures. Besides, we know that the commercial objective lens is a double convex lens. Due to the excellent profile control of our aspheric lens, it could compete with the commercial lens in spot size.

An optical system shown in figure 9 was set up to carry out spot size measurements (shown in figures 7(*a*)–(*d*)). A 405 nm laser diode with a power of 8.5 mW was used as the light source. In this system, a numerical aperture (NA) of the 0.1 (4×) microscope objective lens was used as a spatial filter and to ensure that the measurement would not introduce unwanted aberrations. Next, a pinhole (40 μm) was used to filter out redundant high-frequency noise. The light was directed to the aspheric lens. A neutral density filter was used in order to avoid the CCD (Watec WAT-221 S, pixel size

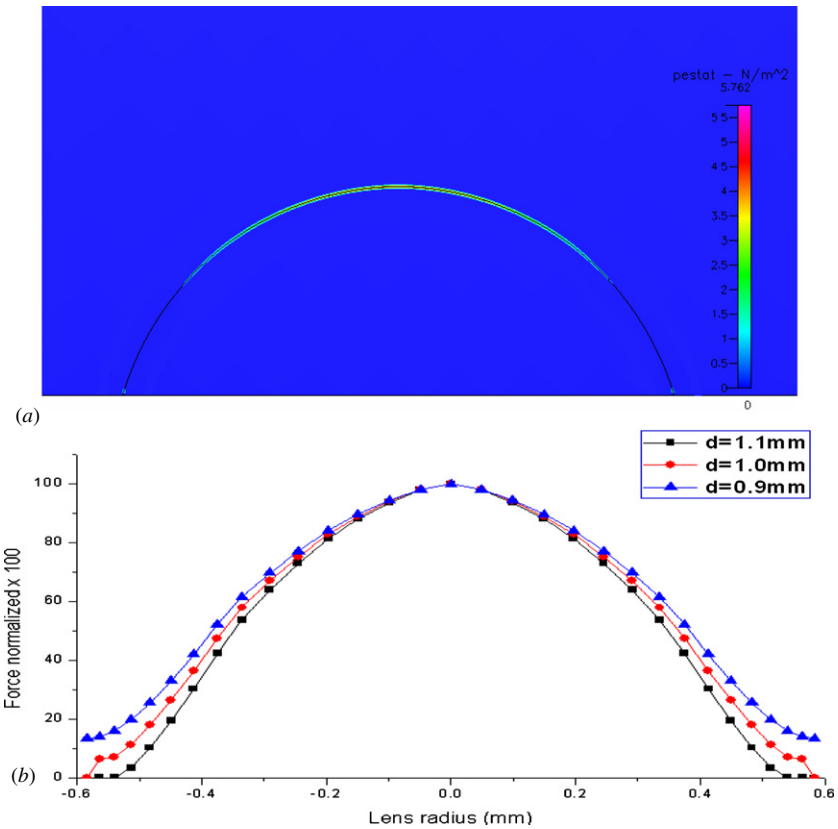

Figure 4. (*a*) Simulation results of the electric field by CFDRC. (*b*) Distribution profile of the gradient electrostatic force for different *d*.

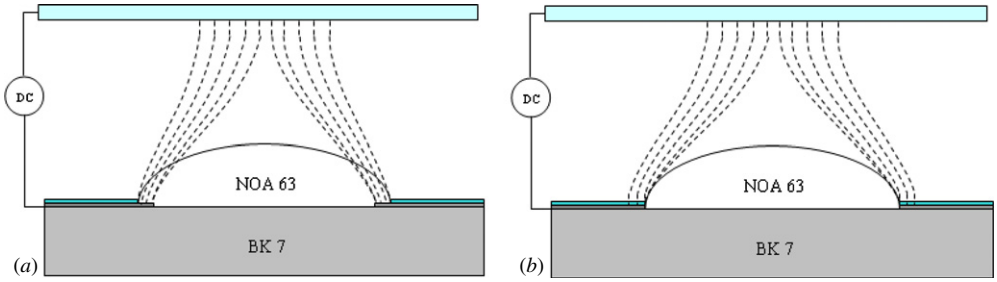

Figure 5. The concept of electrostatic force distribution for (*a*) $d = 0.9 < D$ and (*b*) $d = 1.1 \sim D$.

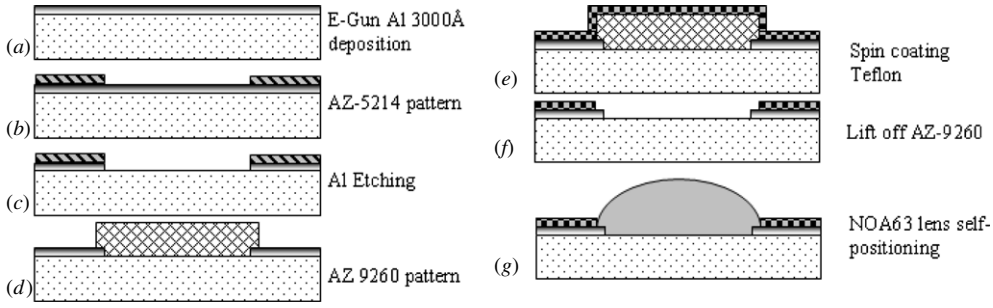

Figure 6. The fabrication process of the bottom electrode.

8.4 μm(H) $\times$ 9.8 μm(V)) saturation. In addition, in order to improve the optical system resolution, we used a 100$\times$ magnification long-working distance lens before the CCD. Image processing software (Image-Pro Plus Program) was used to calculate the pixels of the optical energy distribution and to analyze the FWHM of the spot size.

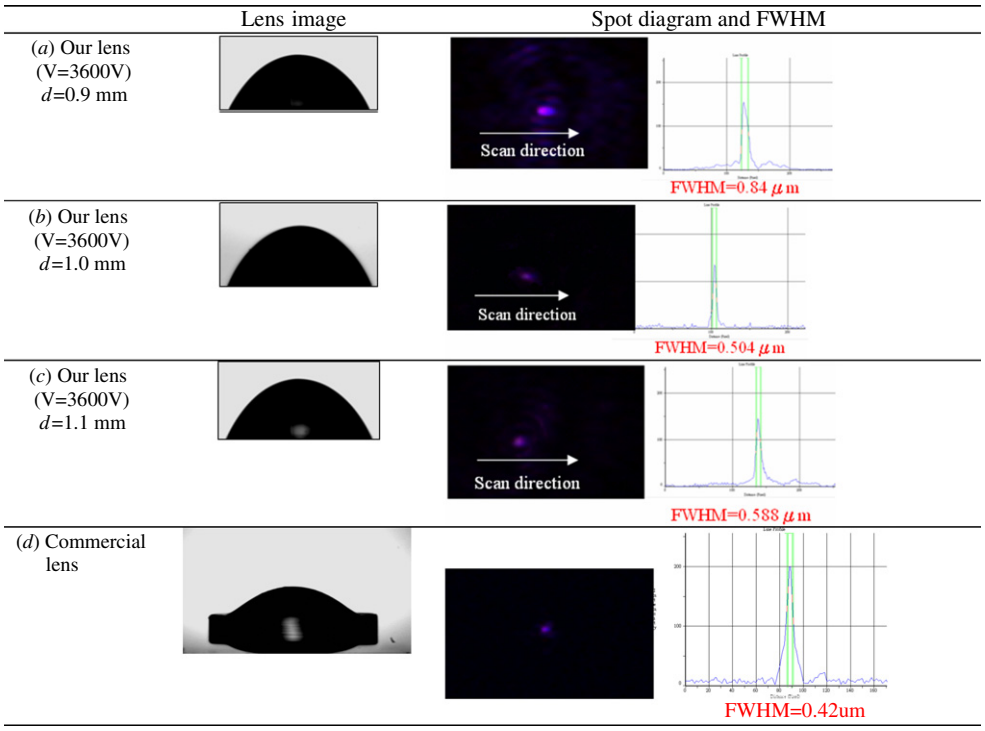

Figure 7. Lens images for *d* values of (*a*) 0.9, (*b*) 1.0, (*c*) 1.1 mm and (*d*) commercial lens and their spot sizes, respectively.

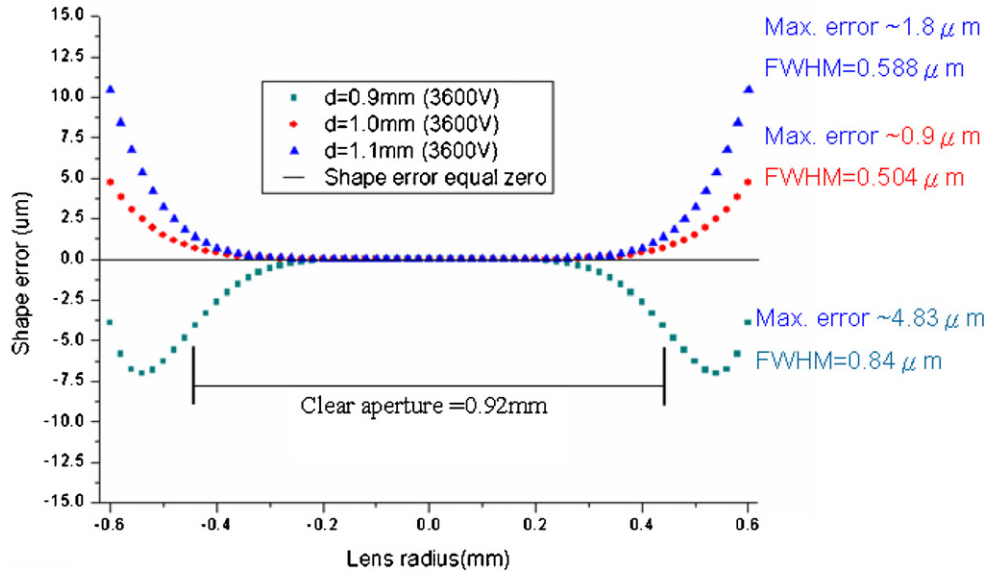

Figure 8. The shape error of the lens (compared to the design profile given in equation (1)) obtained by curve fitting.

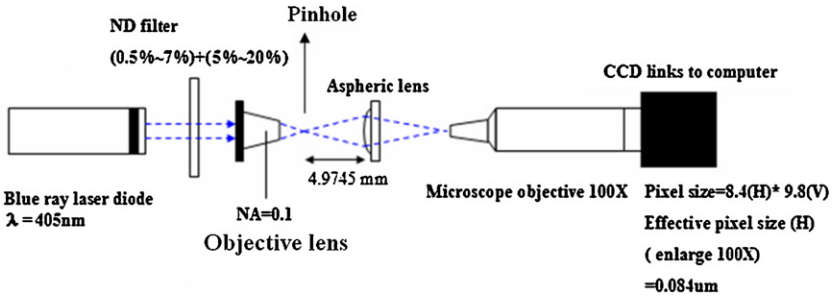

Figure 9. System setup used to measure the spot size of the aspheric lens.

Conclusions

In this paper, we successfully demonstrated the capability of fabricating microlenses by employing a gradient electrostatic potential and a novel electrode design. The study successfully used a hybrid structure and electrostatic force to fabricate aspheric lenses with high transmittance (95% at 405 nm). The hybrid structure was composed of Norland Optical Adhesive 63 (NOA63) (refractive index: 1.5802 at 405 nm) and BK-7 glass (refractive index: 1.5302). OSLO and CFD software packages were used to simulate gradients of the electric field between top and bottom electrodes and assist the optimum bottom electrode design. Different electrode designs were also tested in order to optimize the morphology of the lens profile design. The optimum lens parameters were obtained with $d = 1.0$ mm at 3600 V and the electrode spacer was 3 mm. The resulting lenses have a clear aperture of approximately 0.92 mm, the maximum shape error is less than 0.18%, and the spot size of the fabricated aspheric lenses can be controlled to approximately 0.504 μm ($\lambda = 405$ nm). This technique compares favorably to plastic injection molding aspheric lens manufacturing process where the use of a precision mold can be avoided as well as demolding and stress problems. This technology could be used as a generic approach to fabricate lenses for applications in various micro-optical systems.

Acknowledgment

We would like to thank the Ministry of Economic Affairs of Taiwan for supporting the project budget, under grant number 96-EC-17-A-07-S1-011.

References

[1] Heckele M and Schomburg W K 2004 Review on micro molding of thermoplastic polymers *J. Micromech. Microeng.* **14** R1–14

[2] Su Y C, Shah J and Lin L W 2004 Implementation and analysis of polymeric microstructure replication by micro injection molding *J. Micromech. Microeng.* **14** 415–22

[3] Moon S D, Lee N and Kang S 2003 Fabrication of microlens array using micro-compression molding with an electroformed mold insert *J. Micromech. Microeng.* **13** 98–103

[4] Hung K Y, Tseng F G and Liao T H 2008 Electrostatic force modulated micro-aspherical lens for optical pickup head *J. Microelectromech. Syst.* **17** 370–80

[5] Kuiper S and Hendriks B H W 2004 Variable-focus liquid lens for miniature cameras *Appl. Phys. Lett.* **85** 1128–30

[6] Cheng C C, Chang C A and Yeh J A 2006 Variable focus dielectric liquid droplet lens *Opt. Express* **14** 4101–6

[7] Vallet M, Berge B and Volvelle L 1996 Electrowetting of water and aqueous solutions on poly(ethyleneterephthalate) insulating films *Polymer* **37** 2465–70

[8] Cheng C C and Yeh J A 2007 Dielectrically actuated liquid lens *Opt. Express* **15** 7140–5

[9] Ren H and Wu S T 2008 Tunable-focus liquid microlens array using dielectrophoretic effect *Opt. Express* **16** 2646–52

[10] Ren H, Xianyu H, Xu S and Wu S T 2008 Adaptive dielectric liquid lens *Opt. Express* **16** 14954–60

[11] Xu S, Lin Y J and Wu S T 2009 Dielectric liquid microlens with well-shaped electrode *Opt. Express* **17** 10499–505

[12] William T K 1872 *Reprint of Papers on Electrostatics and Magnetism by William Thomson Kelvin* (London: Macmillan)